Preparation of Recyclable and Versatile Porous Poly-Arylthioethers by Reversible Pd-Catalysed C–S/C–S Metathesis

Miguel A. Rivero-Crespo, Georgios Toupalas and Bill Morandi*

ETH Zürich, Vladimir-Prelog-Weg 1-5/10, 8093 Zürich, Switzerland

porous materials, catalysis, metathesis, polymer chemistry, recyclable

---

ABSTRACT: Porous organic polymers have shown a number of promising properties; however, their application is usually hampered due to the lability of their linkages. Inspired by the outstanding chemical, mechanical and thermal resistance of the 1D polymer polyphenylene sulphide (PPS), we have designed a new family of 2D and 3D poly-arylthioethers, synthesised *via* a mild Pd-catalysed C–S/C–S metathesis-based method, that merges the attractive features common to porous polymers and PPS in a single material. In addition, the method is highly modular, allowing to easily introduce application-oriented functionalities in the materials for a series of environmentally relevant applications including metal capture, metal sensing and heterogeneous catalysis. Moreover, despite their extreme chemical resistance, the polymers can be easily recycled to recover the original monomers, offering an attractive perspective for their sustainable use. In a broader context, these results clearly demonstrate the untapped potential of emerging single-bond metathesis reactions in the preparation of new, recyclable materials

---

INTRODUCTION

Porous organic materials, including amorphous polymers and covalent organic frameworks (COFs), are a privileged class of materials with high surface area, low mass density, and modular topology that have gathered a lot of attention among the chemistry and materials science communities during the last two decades.[1-9] They have shown promising applications spanning areas from gas and metal capture, to optoelectronics and catalysis, among others.[10-14] Dynamic covalent chemistry (DCC)[15] is a key feature in the synthesis of these systems; the reversibility of the reactions provides self-correcting behaviour which, in turn, allows the formation of high-quality, low-defect materials. Despite their interesting properties, the lability of most of the linkages (e.g. imine, boronate ester, boroxine) used to construct these materials under self-correcting conditions makes them unstable towards moderately harsh media (e.g. water, pH, temperature, pressure), often hampering their industrial application. For this reason, the synthesis of analogous yet more stable materials containing stronger covalent bonds in a DCC-like manner is highly attractive. Ideally, such new materials should, despite their high chemical strength, be recyclable to their monomers to allow for their circular use in accordance with sustainable chemistry goals.[16] Sulphur containing 1D-polymers like polyphenylene sulphide (PPS) have seen widespread use in industry as insulators and replacements for metal parts due to their extremely high chemical, thermal and mechanical resistance, as illustrated by the large number of patents (>100’000) in this area.[17,18] However, the harsh conditions required for their synthesis (Scheme 1a, polycondensation > 250 °C, Na_2S, autogenous pressure)[17,19] and the extreme stability of the thioether bonds, make it difficult to fine-tune PPS’s properties (M_w, cross-linking, polydispersity, etc.). Moreover, this dramatically limits the possibility to access more complex poly-arylthioether-based structures with 2D or 3D cores, despite their potential to exhibit advanced features such as porosity, metal-binding ability or optoelectronic properties, among others. The synthesis of such advanced materials, which should be analogous to PPS in terms of chemical, thermal and mechanical stability, would be a step forward towards the industrial application of porous polymers. Among the extremely scarce examples of porous poly-arylthioether-based materials,[20,21] Swager and co-workers reported the synthesis of thianthrene-based 2D polymers with high surface area and interesting redox properties using dynamic S_NAr reactions of thiocatechols and perfluorinated aromatic compounds (Scheme 1b).[22] While this synthetic method provides an exciting new approach, it is limited to specific monomers (1,2,4,5-benzenetetrathiol with hexafluorobenzene or octafluoronaphtalene) that can participate in the S_NAr reaction. Moreover, potential applications of these materials have not yet been extensively explored and their recyclability has not been demonstrated. Therefore, there is a critical need to develop new, complementary approaches to fully harness the potential of porous poly-arylthioethers in advanced materials and catalytic applications with a focus on sustainability.

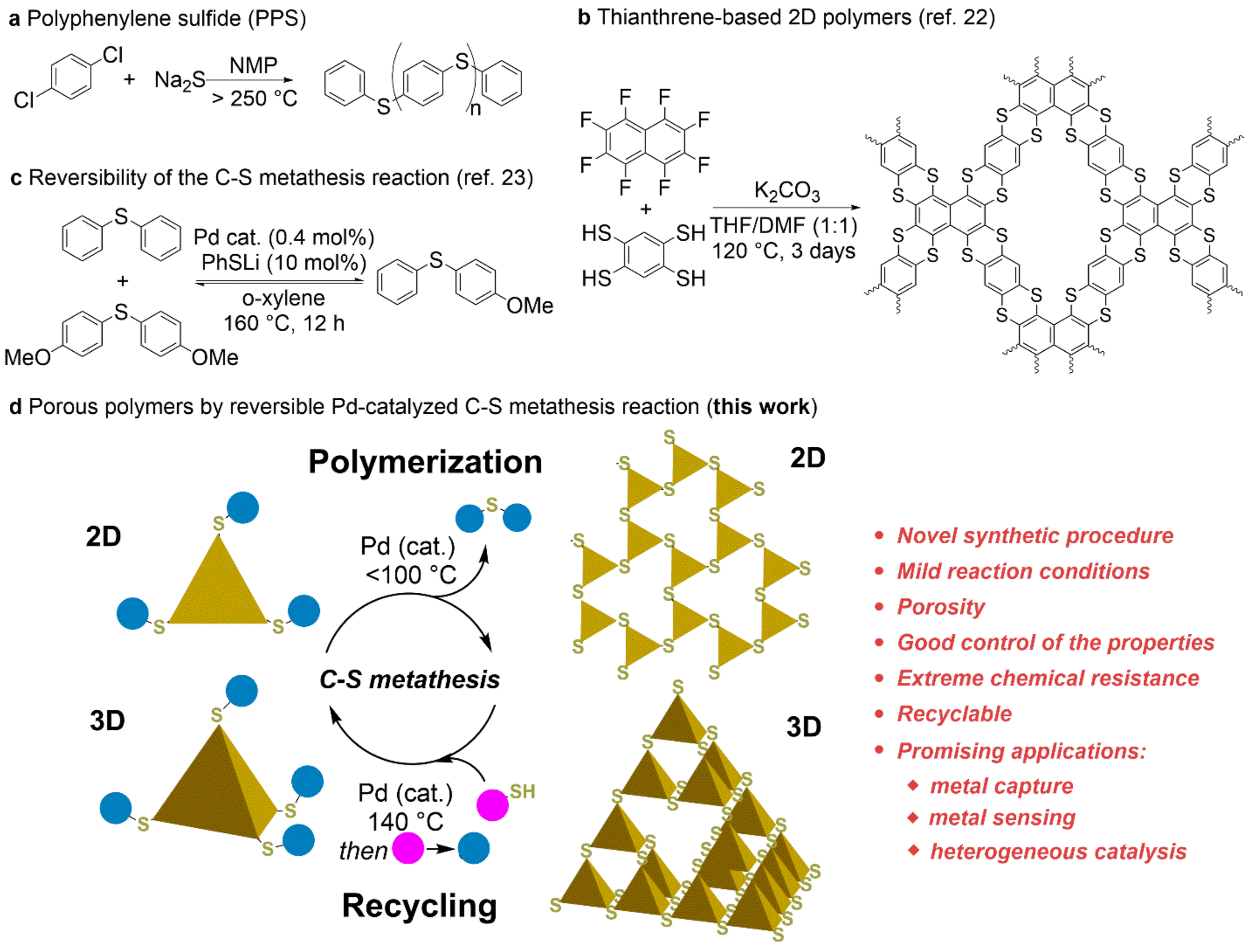

Scheme 1. Synthesis and structure of **a** PPS and **b** thianthrene-based 2D polymers. **c** Experiment showing the reversibility of the C–S/C–S metathesis reaction: equilibrium is reached starting from both sides. **d** Approach followed in this work.

Our group has previously developed transition-metal-catalysed C–S/C–S single-bond metathesis reactions and showcased their utility in small molecule synthesis.[23,24] These reactions allow the facile synthesis of a number of thioether molecules and macrocycles from the corresponding thiols as nucleophiles and aryl–SR (R = H, Me) compounds as electrophiles by driving the equilibrium towards product formation (excess of nucleophile and precipitation of LiSMe or Li_2S salts). Interestingly, depolymerisation of PPS was achieved in 85% yield, showing the potential of the reaction for polymer recycling.[23] In addition, full reversibility was demonstrated at high temperatures (160 °C) by scrambling of the aryl groups giving a statistical mixture of products both in the forward and reverse reactions (Scheme 1c). As mentioned previously, full reversibility of the reaction is highly desirable for materials synthesis in order to obtain high quality polymers with fine-tuned properties and open the door for the material's recycling after use. While transition metal catalysis is widely applied to make conventional 1D polymers, including reversible reactions such as olefin metathesis,[25,26] their use in the synthesis of 2D and 3D porous polymers is much less developed. Some remarkable examples include the report from Dichtel and co-workers using catalytic amounts of metal triflates to make imine-COFs,[27] or the use of alkyne metathesis by Zhang and co-workers[15,28,29]. For all these reasons, we decided to harness the potential of the reversible Pd-catalysed C–S/C–S metathesis reaction to not only synthesise 2D and 3D-porous polymers, but also to readily recycle them after use. Herein, we report the synthesis of a new family of arylthioether-based porous organic polymers from simple building blocks enabled by a fully reversible version of the Pd-catalysed C–S/C–S metathesis reaction with exquisite control over the physical properties of the resulting materials (Scheme 1d). Importantly, the materials can be recycled to the monomers and reveal promising applications in metal capture, metal sensing and heterogeneous catalysis.

RESULTS AND DISCUSSION

Preliminary kinetic study. Translating a reversible catalytic reaction from small molecule synthesis to materials preparation is a daunting task encompassing many challenges such as catalyst deactivation and insufficient self-correcting ability due to unfavourable kinetics. In this context, our previous work showing one example of the fully reversible C–S/C–S metathesis of diarylthioethers at high temperatures (160 °C) needed careful re-evaluation.[23] Under such harsh conditions, side reactions and catalyst decomposition become problematic and can hamper the synthesis of the materials. In order to address these issues, we studied the effect of the electronic properties on the reaction rate by performing a 2D-Hammett analysis using various symmetric arylthioethers with different substituents. Interestingly, the reaction is extremely fast, even at much lower temperatures than previously reported (80 vs. 160 °C), in a small, optimal range of matching electronic properties (Figure 1a and S1, $-0.2 < \sigma(Ar_1 \text{ and } Ar_2) < 0.2$). We can thus conclude that the design of the optimal building blocks should rely on electronically neutral, minimally biased aromatic monomers. Noteworthy, the C–S/C–S metathesis reaction rate is in the same order of magnitude as imine condensation used for COFs synthesis (70 °C, 3.0 vs. 10.0 $mM \cdot min^{-1}$, respectively, Figure S2),[30] which further supports its potential in the synthesis of materials following a DCC approach. We also evaluated the effect of different parameters on the rate and catalyst lifetime in order to find the optimal range of conditions for the reaction. In particular, temperature has a big influence on catalyst stability: the catalyst does not show significant deactivation up to 100 °C but deactivates readily at higher temperatures (Figure 1b, see Table S1 and Figure S3 for the full study).

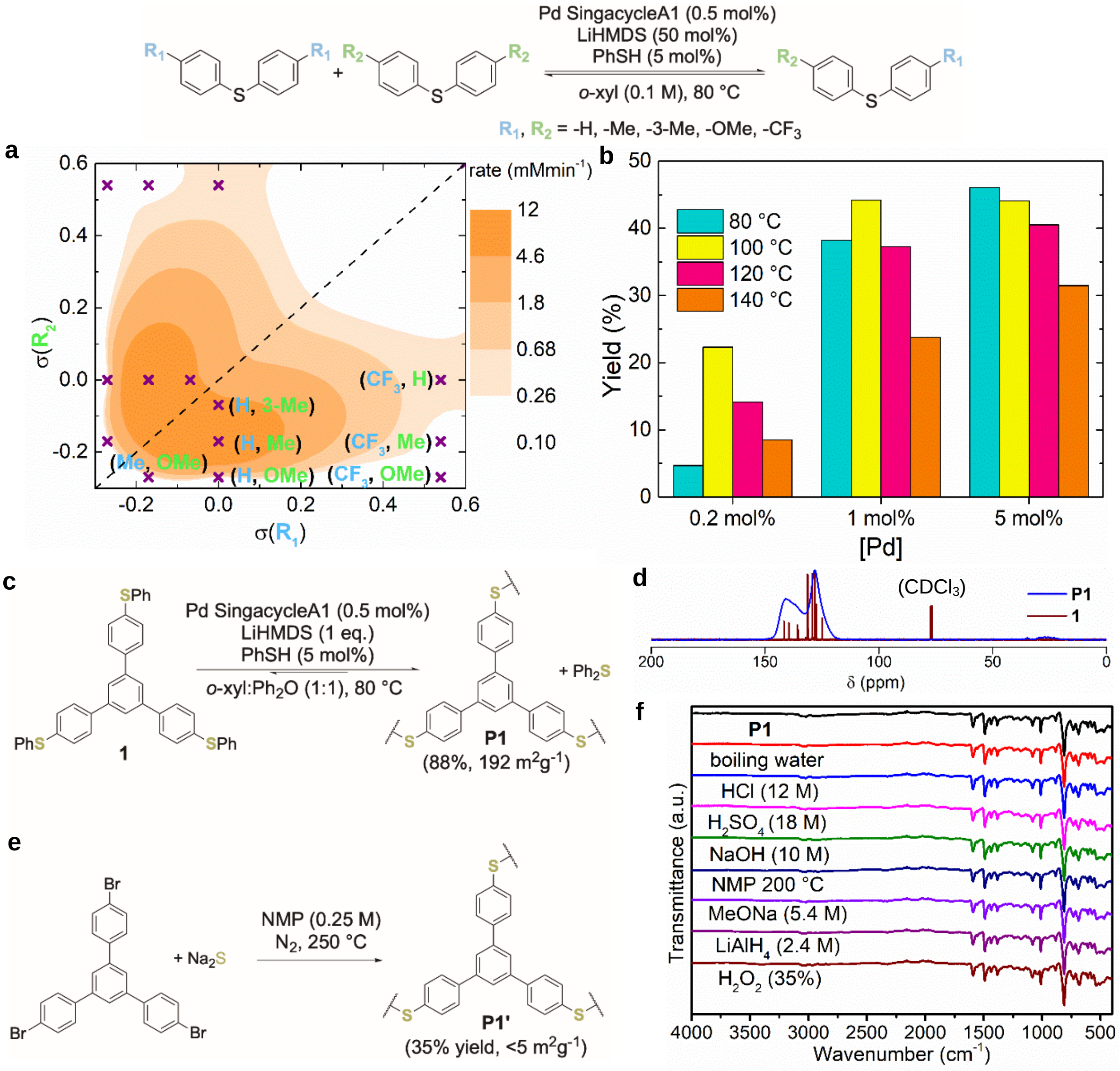

Figure 1. Preliminary mechanistic studies. **a** Kinetics of C–S/C–S metathesis (top) in the scrambling of aryl groups with different electronic properties. Note the logarithmic scale for the contour plot. **b** Yield for the model reaction (benzyl phenyl sulphide + 3-trifluoromethyl thioanisole) after 16 hours as a function of [Pd] and reaction temperature. **c** Synthesis of a model poly-arylthioether **P1** by reversible C–S metathesis reaction. Values in parentheses show yield by mass and surface area of the polymers. **d** Solid state ^{13}C CP-MAS NMR spectra of **P1** and liquid ^{13}C NMR spectra of the monomer **1** ($CDCl_3$). **e** Synthesis of **P1'** *via* non-reversible polycondensation reaction. Values in parentheses show yield by mass and surface area of the polymers. **f** FT-IR spectra of **P1** after 24 hours in contact with different chemicals.

Synthesis and characterisation of the polymers. Using the information gathered from the preliminary kinetic experiments, we designed the model monomer **1** containing an 1,3,5-triphenylbenzene core with D_{3h} geometry bearing 3 electronically neutral phenyl thioether functional groups. The optimal polymerisation conditions were found by performing a screening within the narrow set of conditions obtained from the preliminary kinetic study ([**1**], [PhSH], [LiHMDS], [Pd], T, solvent and stirring, Table S2). With the optimised conditions in hand, we performed the gram-scale synthesis of **P1** in excellent yield (Figure 1c), in good agreement with the conversion measured as yield of by-product (Ph_2S) by GC analysis (Table S7). In addition, FT-IR shows the disappearance of the bands associated with the pendant –SPh groups of the monomers (Figure S17). Elemental analysis of the synthesised structure showed good agreement between the measured and calculated amount of C, H and S (Table S8). As expected, controls performed without Pd catalyst or base gave neither solid formation nor conversion. These results are remarkable, as examples of reversible, metal-catalysed syntheses of porous materials are scarce in the literature.[27-29] The choice of the solvent system is extremely important in the synthesis of porous polymeric structures: stabilisation of oligomers and formation of colloids in the solution during the first stages of the reaction is proposed to prevent a premature precipitation of the particles, ensuring continuous growth and self-correction which lead to low-defect materials.[31] We decided to use Ph_2O as co-solvent due to its ability to partially solubilise PPS[32] (Figure S4). Indeed, using a one-to-one mixture of *o*-xylene/Ph_2O as solvent, **P1** was obtained as a colloidal suspension after 20 hours, in contrast to pure *o*-xylene that formed a precipitate, confirming the stabilising effect of Ph_2O (in both cases, turbidity appeared after 20 minutes). Field emission scanning electron microscopy (FESEM) showed a remarkable difference in **P1** particle size for both solvent systems (50 vs. 200 nm, for *o*-xylene/Ph_2O and *o*-xylene, respectively, Figures S38 and S43). Moreover, the surface area of **P1** was reduced from 192 $m^2 \cdot g^{-1}$ for *o*-xylene/Ph_2O to 66 $m^2 \cdot g^{-1}$ for *o*-xylene (Figures S29 and S30). Temperature had also a big impact on the surface area (192 vs. 36 $m^2 \cdot g^{-1}$ for 80 and 120 °C, respectively, Figures S29 and S31) and particle size (50 vs. 500 nm for 80 and 120 °C, respectively, Figures S38 and S44). Thus, by modification of the temperature and the solvent system, we were able to control the physicochemical properties of the material.

Inductively coupled plasma optical emission spectroscopy (ICP-OES) measurements of the digested polymers detected some remaining Pd in the polymers even after washing the solids with a chelating agent (1,3-propanodiamine, Table S9).[33] The Pd remaining in the structure is likely to be trapped in closed pores and stay inaccessible to the chelating agent under such conditions. Pd-K edge extended X-ray absorption fine structure (EXAFS) measurements of the materials synthesised employing different reaction conditions showed that the remaining metal embedded within the structure is coordinated to sulphur (R = 1.8 Å) and carbon (R = 1.4 Å) atoms, which most likely corresponds to the oxidative addition product of the Pd into the Ar–S bond (Figures S65 and S66). This observation points towards transmetallation as the rate-determining-step on the reaction.[34]

To demonstrate the importance of the reaction's reversibility for the synthesis of the materials, an alternative synthesis of the material **P1** was attempted following the most common procedure to prepare sulphur-based polymers: polycondensation reaction of aryl halides with Na_2S at elevated temperatures (250 °C). The material **P1'** was indeed obtained according to the FT-IR spectra (Figure S22), albeit in considerably lower yield than **P1** (35% vs. 88%, Figure 1e) and, more importantly, **P1'** was non-porous ($<5\ m^2 \cdot g^{-1}$ vs $192\ m^2 \cdot g^{-1}$ for **P1**), indicative of an amorphous, interlinked polymer formed under complete kinetic control. These results highlight that, while the standard polycondensation reaction can somewhat enable the low-yielding formation of a similar structure, the reversibility of the C–S/C–S metathesis is a crucial factor in the synthesis of these materials providing a higher degree of local ordering through self-correction as evidenced by the formation of pores and the well-defined particle sizes, two important features for downstream applications.

Chemical resistance of the material **P1** was tested by immersion in different solutions for 24 hours: boiling water, NMP at 200 °C, strong acids, bases, reducing agents and oxidizing agents and the FT-IR spectra before and after exposing the materials to these conditions were compared (Figure 1f). Very small differences were observed between the spectra (see Figure S23 for subtracted spectra), demonstrating the extremely high stability of the materials against harsh chemicals and conditions, comparable to poly-arylether-based COFs.[35] Moreover, adsorption isotherms of **P1** after 24 h contact with the harshest chemicals according to the FT-IR spectra: H_2SO_4 (18 M) and H_2O_2 (35% v/v), showed that most of the porosity is retained (Figures S32, S33 and Table S12), as well as the mass balance (98% and 80%, respectively), further confirming the exceptional chemical stability of the porous poly-arylthioethers.

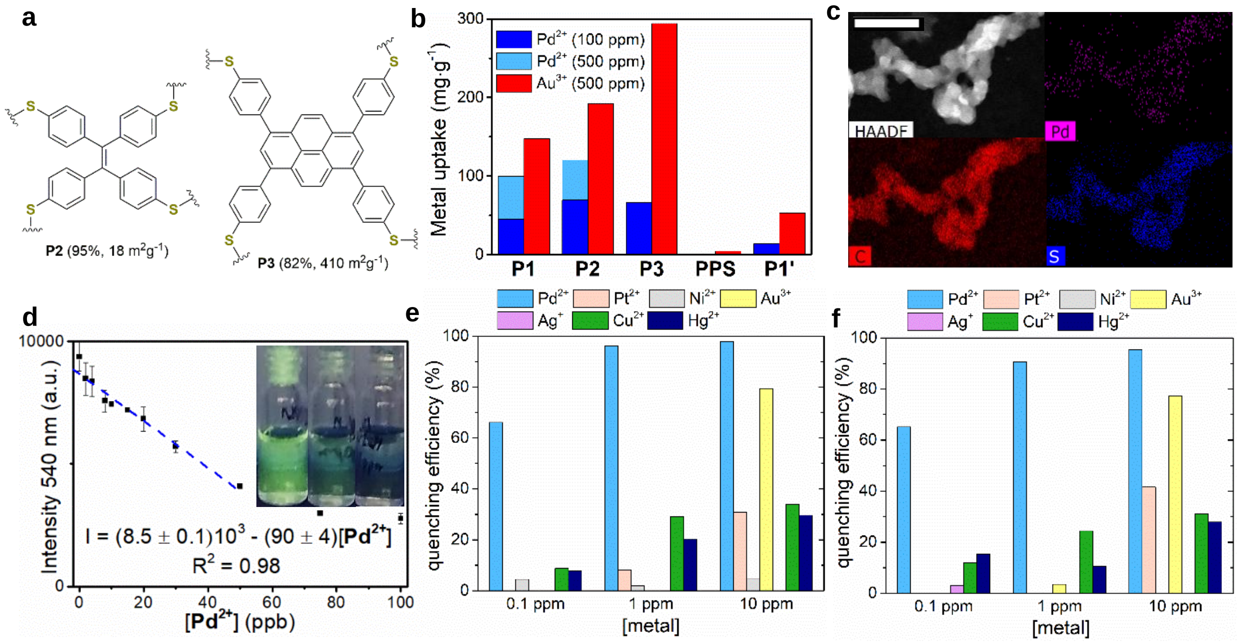

Figure 2. **a** Structures of the polymers **P2** and **P3**. Values in parentheses show yields by mass and surface area. **b** Pd^{2+} and Au^{3+} uptake capacity from aqueous solutions containing $PdCl_2$ (100 or 500 ppm) and $AuCl_3$ (500 ppm). **c** HAADF image and EDX mapping of Pd^{2+}@**P1** (1 wt%, bar represents 200 nm). **d** Fluorescence emission intensity of **P2** in water (2 ppm) at 540 nm (excitation at 370 nm) vs. $[Pd^{2+}]$. Inset shows the quenching of fluorescence in a dispersion of **P2** (10 ppm) after adding Pd^{2+} (from left to right 0, 0.1 and 1.0 ppm). **e** Fluorescence quenching of **P2** (10 ppm) by different metal cations (0.1, 1.0 and 10 ppm). **f** Fluorescence quenching of **P3** (10 ppm) by different metal cations (0.1, 1.0 and 10 ppm).

Design of fluorescent polymers for noble metal sensing and capture. Given the simplicity and mild conditions of our synthetic method, we hypothesised that using monomers containing different functionalities, we could easily access a variety of new functional materials. One straightforward application for porous, sulphur-containing materials would be in detection and capture of noble metals from water. Water contamination by noble metal cations is an environmental challenge due to its harmful effects on human health and ecosystems.[36] In addition to that, efficient recovery of expensive metals like Pd, Au and Pt from industrial waste waters can have a huge economic impact due to their scarcity and high price. The porosity of the polymers and the high density of sulphur atoms (10-20 wt%) with high affinity for noble metals can enable the capture of the metal ions from water, while a built-in fluorescent functionality can potentially enable metal sensing by fluorescence-quenching, one of the methods of choice to detect metal cations in aqueous solutions due to its high sensitivity.[37-39] Indeed, several porous materials have already been used for metal capture including MOFs,[40] COFs[41] and polymers[42].

Two new polymers **P2** and **P3** were synthesised containing well-studied fluorophore cores including tetraphenylethylene and tetraphenylpyrene, respectively (Figure 2a).[43,44] Both polymers were synthesised in high yields and **P3** displays a high surface area, in accordance with the high rigidity of the monomer core. We evaluated the capacity of **P1-3** for Au^{3+} and Pd^{2+} capture, two common and valuable pollutants in industrial wastewaters (Figure 2b). In the case of palladium, the materials were able to capture up to 69 $mg\cdot g^{-1}$ of Pd^{2+} from a 100 ppm $PdCl_2$ solution, which could be increased to 115 $mg\cdot g^{-1}$ starting from a 500 ppm $PdCl_2$ solution. The amount of Au captured by the polymers from a 500 ppm $AuCl_3$ solution was up to 295 $mg\cdot g^{-1}$, which corresponds to almost 50% of sulphur atoms in the structure coordinated to Au. The material **P2** showed the highest capacity for Pd^{2+} and **P3** for Au^{3+}. Importantly, most of the metal cations could be easily removed from the solids by washing with 1,3-diaminopropane in NMP and **P1** could be reused to almost 100% capacity over three cycles (Figure S7). **P1'** and commercial PPS on the other hand, showed much lower capacity for metal uptake, further highlighting the importance of our synthetic method with regard to the polymers properties and applications.

We next sought to experimentally confirm that the structural thioether groups are indeed responsible for the metal binding properties of the material. High-resolution transmission electron microscopy (HR-TEM) and high-angle annular dark-field (HAADF) coupled to EDX images showed the good dispersion of the metals in the material (Figure 2c). Pd-K edge EXAFS measurements indicated that the absorbed Pd^{2+} is directly bound to the sulphur sites (R = 1.8 Å) with different degrees of hydration[45] (R = 1.5 Å, Figure S67). Moreover, the Pd^{2+} uptake capacity was not affected by different amounts of PhSH in the synthesis of **P1** (69.3, 69.0 and 72.3 $mg\cdot g^{-1}$ respectively for 2, 5 and 10 mol% of PhSH), clearly pointing towards structural thioethers, and not residual thiols, acting as binding sites. In contrast to our new materials, commonly used metal absorbents based on porous materials traditionally rely on pendant thiol groups in order to adsorb higher amounts of metals.[40,41] However, these free thiols have to be introduced in an additional post-synthetic modification step that significantly increases the complexity of the material's preparation. In addition, the strong metal-thiol interaction makes it difficult to recover the metals from the solid without damaging the structure.

Notably, both materials **P2** and **P3** were extremely sensitive for Pd^{2+} detection, with **P2** being able to sense down to 2 ppb or 0.019 μM (Figure 2d), making it considerably more sensitive than other solid materials like polymers[46] or MOFs[47] (400 and 44 ppb of Pd^{2+}, respectively) and are even at the level of the best small molecule sensors reported.[48] Moreover, the response was fast (within seconds) and both materials were extremely selective for Pd^{2+}; the fluorescence was not significantly affected by other cations such as Pt^{2+}, Cu^{2+}, Ni^{2+}, Ag^{+} or Hg^{2+} (Figures 2e, 2f, S8-S13) and just slightly by Au^{3+} – 10 ppm of Au^{3+} induces similar response as 0.1 ppm of Pd^{2+} – demonstrating the great potential of the materials as very sensitive and selective sensors for Pd^{2+} traces in water.

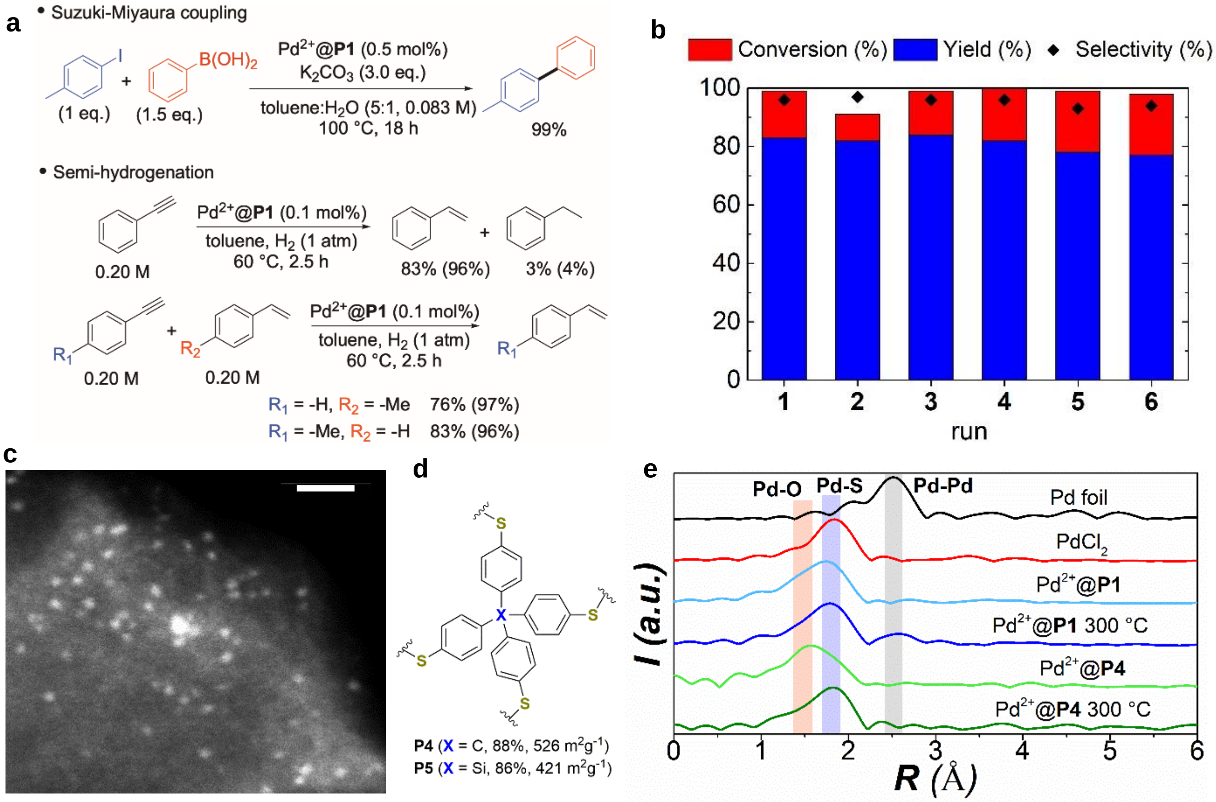

Figure 3. a Reactivity of the Pd^{2+}@**P1** (1 wt% Pd) as heterogeneous catalyst. Yields are shown and values in parentheses stand for selectivity of semi- vs. complete hydrogenation. **b** Reusability of Pd^{2+}@**P1** over 6 cycles of phenylacetylene semi-hydrogenation. **c** HAADF image of Pd^{2+}@**P1** after Suzuki reaction (bar represents 10 nm). **d** Structures of the polymers **P4** and **P5**. Values in parentheses show yield by mass and surface area. **e** k^2-weighted Fourier transform of the EXAFS function for Pd^{2+}@**P1** and Pd^{2+}@**P4** at RT and 300 °C under H_2 stream and selected references. Pd-O interaction is due to the hydration of the Pd^{2+}.

Expansion to 3D geometries and catalytic application of Pd^{2+}@P1/P4. Given the high capacity of the polymers to adsorb and disperse noble metals, we decided to test the hybrid material Pd^{2+}@**P1** (1 wt% Pd) as heterogeneous catalyst. One of the key features of a good catalyst support is the ability to stabilise metals without binding too strongly and thus reducing catalytic activity. Considering the characteristics of our new materials:

high surface area, good dispersion of the metals and reversible binding to the metal cations; we hypothesised that they could be efficient supports for noble metal catalysts. Similar materials including carbon nitride[49,50] or even PPS[51] have been used as supports to stabilise and modify catalytic activity of Pd in catalysis. Gratifyingly, Pd^{2+}@**P1** showed good catalytic activity for classical Pd-catalysed reactions, i.e. Suzuki-Miyaura coupling and the industrially relevant semi-hydrogenation of terminal alkynes (Figure 3a).[52] Notably, Pd^{2+}@**P1** could perform the semi-hydrogenation of phenylacetylene to styrene under mild conditions with high selectivity (>95%) and can be reused over 6 cycles (TON = 5860) without significant loss of activity (Figure 3b). Moreover, the hot-filtration test showed that the Suzuki and semi-hydrogenation reactions stopped when the solid was filtered from the solution (Figure S14 and S16), indicating that the reaction takes place in the solid/liquid interface and not in the solution by leaching of metal species. Control experiments without catalyst or using the as-synthesised and the washed materials prior to supporting Pd^{2+} did not give any activity, confirming that the structural Pd atoms (analysed by ICP-OES) are not accessible to the reagents under the reaction conditions. HR-TEM and EXAFS after the Suzuki and hydrogenation reactions show that the support is able to prevent agglomeration of Pd, and only small amounts of subnanometer Pd clusters were detected (Figure 3c).

Analogously as previously done for the fluorophores in **P2** and **P3**, harnessing the versatility of the reaction, we can design monomers with T_d geometry in order to expand the family of porous poly-arylthioethers to 3D structures. These structures can be ideal supports for single atom catalysts (SACs) due to their presumably higher porosity than the corresponding 2D analogues, providing better stabilization of the metals and improved diffusion of the reactants and products under reaction conditions. We designed the polymers **P4** and **P5** (Figure 3d) containing tetraphenyl methane and silane, respectively. These materials were synthesised in excellent yields and, in fact, showed the highest surface areas of all the family. We compared **P1** and **P4** as supports for single atom catalysts (SACs) under reducing gas-phase reaction conditions (H_2 atmosphere, up to 400 °C). Pd-K EXAFS in-situ measurements of Pd^{2+}@**P1** and Pd^{2+}@**P4** (1.0 and 0.6 wt% Pd^{2+}, respectively) suggested that the materials were able to stabilise and isolate the Pd atoms, preventing agglomeration even up to 300 °C under H_2 atmosphere (Figure 3e) – only a small Pd-Pd contribution appears for **P1**, whereas no Pd-Pd feature appears for **P4**, consistent with the higher surface area of the latter. X-ray absorption near edge structure (XANES) region indicates reduction of the Pd already at 100 °C (Figure S68 and S69).[53] These results reinforce the potential of the sulphur-containing porous polymers as supports for gas-phase heterogeneous catalysts. Further reactivity tests are underway in our laboratories to unlock the full potential of this new family of materials in catalysis.

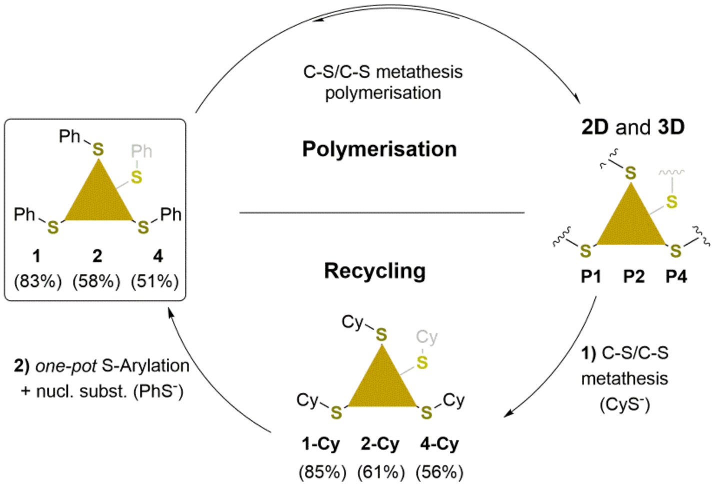

Figure 4. Recyclability of the polymers to the initial monomers. Percentages in parenthesis indicate isolated yields starting from the polymers.

Recyclability of the polymers. Being able to recycle polymeric materials to the original monomers at the end of their life-cycle is one of the biggest challenges in sustainable chemistry. Decomposition and revalorization of polymers have been extensively studied in the last decades, however, recovery of the original monomers from the polymers is still rare and usually requires the design of polymers that are labile under acidic conditions (ester, amide, etc.).[54] Moreover, despite some relevant efforts to depolymerise linear polymers synthesised by reversible alkyne metathesis to macrocycles;[55,56] recovery of the original monomers from porous polymers has not yet been demonstrated. Given the extraordinary chemical stability of the porous poly-arylthioethers reported in this work, recycling them to the monomers poses an evident challenge, however, since they were synthesised by a reversible reaction, the same reaction should give the monomers back under suitable conditions. Unfortunately, the C–S metathesis reaction with excess of thiophenol was not effective to directly recycle the polymers, probably due to the low reactivity of the thiophenol towards transmetallation that kinetically prevents any efficient degradation. Gratifyingly, when using a more nucleophilic thiol, cyclohexanethiol, the polymers **P1**, **P2** and **P4** could all be readily depolymerised in high yields to a close analogue of the original monomer (Figure 4). Subsequent S-arylation *via* diphenyliodonium hexafluorophosphate led to the formation of the corresponding sulfonium salts, which were reacted in one pot with thiophenol in a nucleophilic substitution reaction, yielding the original monomers through a direct Cy- to Ph- switch. This demonstrates how, thanks to transition metal catalysis, polymeric materials can be designed to be extremely stable and, at the same time, be easily recycled back to the starting monomers.

CONCLUSIONS AND OUTLOOK

We have developed a new methodology to synthesise previously unknown porous polymers linked by strong thioether bonds, which would be difficult to access by traditional synthetic methods, by using the reversible Pd-catalysed C–S/C–S metathesis reaction. The materials were obtained in good yields, with high surface areas and are extremely resistant against several harsh conditions including highly reactive chemicals. We have demonstrated the importance of the reaction's reversibility in order to produce high quality materials and good control over their properties. In addition, the polymers are highly modular, as several functionalities can be introduced and the materials could be applied in different environmentally relevant fields: metal capture, metal sensing and heterogeneous catalysis, both in liquid and gas phase. In particular, **P2** outperforms previously reported materials in Pd^{2+} sensing, detecting down to 2 ppb with great selectivity. Importantly, the polymers have been designed to be recycled after use by degrading them back to the monomers using palladium catalysis, taking advantage of the reaction's reversibility. This conceptual design is highly relevant in the context of a circular economy. Besides these exciting preliminary results, and given the novelty as well as modularity of this family of materials, we believe that many more applications can be developed in different fields such as photo/electrocatalysis or gas capture by introducing new functionalities. In a broader context, we believe this work demonstrates the untapped potential of emerging single-bond metathesis reactions for the synthesis of robust yet recyclable materials.

Methods

All reactions were carried out under argon in oven-dried glassware using anhydrous solvents. All commercially available compounds were used as received from common suppliers (Sigma-Aldrich, Strem Chemicals, Abcr, TCI, Fluorochem, Acros Organics, Alfa Aesar and Apollo Scientific).

NMR spectra were recorded on Bruker AVANCE III 400, Neo 400, Neo 500, or 600 spectrometers at room temperature; the chemical shifts are reported with respect to internal solvent: δH = 7.26 ppm, and δC = 77.16 (t) ppm ($CDCl_3$); δH = 7.16 ppm, and δC = 128.06 (t) ppm (C6D6); δH = 2.50 (p) ppm, and δC = 39.52 (hept) ppm (DMSO-d6). Multiplicities are indicated by s (singlet), d (doublet), t (triplet), q (quartet), p (quintet), h (sextet), hept (septet), m(multiplet), br (broad), or combinations thereof. GC/FID were measured in a Shimadzu GC-2025 (capillary column: Macherey-Nagel OPTIMA 5, 30.0 m× 0.25 mm × 0.25 μm; carrier gas: H_2); To determine GC yields, calibration curves were generated using *n*-dodecane as an internal standard. ^{13}C CP-MAS solid state NMR was recorded on a Bruker AV NEO 400 using a MASDVT 400WB probe.

High-resolution MS (HRMS) were acquired with a Thermo scientific Q-Exactive GC Orbitrap for EI. Bruker Daltonics maXis ESI-QTOF or solariX ESI-FTICR-MS for ESI. Elemental analysis (EA): C, H, and N measurements were performed in a LECO TruSpec Micro instrument. The gaseous combustion products of C (CO_2) and H (H_2O) were quantified by means of infrared spectroscopy. Nitrogen was measured as N_2 with a thermal conductivity detector. Sulphur was measured in a HEKAtech EuroVector instrument by burning the sample at 1000 °C with an excess of O_2. The composition products were chromatographically separated and measured with a thermal conductivity detector. HRMS and EA were performed in the Molecular and Biomolecular Analysis Service (MoBiAS) in the Laboratorium für Organische Chemie at ETH Zürich. Elemental analyses of Pd and Au for all materials were performed by Inductively Coupled Plasma-Optical Emission Spectrometry (ICP-OES) by the Mikroanalytisches Labor Pascher, Remagen.

X-ray powder diffraction patterns (PXRD) were measured in a PANalytical X'Pert Pro diffractometer using Ni-filtered Cu Kα radiation ($\lambda = 0.1541$ nm). Data were recorded in the 2θ range of 2−30° with an angular step size of 0.05° and a counting time of 1.5 s per step. Transmission Electron Microscopy (TEM): The morphology of the samples, as well as metal distribution and metal particle sizes were obtained by high resolution TEM using a FEI Talos F200X instrument. The samples were prepared by dropcasting a dispersion of the polymers on a copper grid coated with carbon film. Scanning Electron Microscopy (SEM): The morphology and particle sizes of the polymers were analysed by field emission scanning electron microscopy (FE-SEM) using a JEOL JSM-7100F instrument. The samples were prepared by dropcasting a dispersion of the polymers on a copper tape film and coated with carbon using a CCU-010 Carbon Coater Safematic instrument.

N_2 physisorption: The specific surface area of the materials and the porosity were measured from a nitrogen physisorption isotherm recorded at -196 °C on a BEL JAPAN BELSORP-mini apparatus. The surface area values were obtained by the BET method. The pore sizes were obtained by the BJH method using the adsorption branch. The samples were dried at 60 °C under N_2 flow for 16 hours and then 2 hours under vacuum at 100 °C.

X-ray Absorption Spectroscopy (XAS): was conducted at the SuperXAS beamline of the Swiss Light Source. The X-ray beam from the 2.9 T superbend was collimated using a Pt-coated mirror, monochromatised using a Si(111) channel cut monochromator, and focused to a spot size of 500×100 μm (horizontal×vertical) using a Pt-coated toroidal mirror. Data were acquired in air from pressed pellets at the Pd K-edge in transmission and fluorescence modes simultaneously using Quick XAS data acquisition mode, using three 15 cm long Ar/N_2-filled ionization chambers for transmission detection and PIPs diode for fluorescence detection. The samples were placed between the first and the second ionisation chamber. For the absolute energy calibration, a Pd foil was measured simultaneously between the second and a third ionisation chambers. The resulting data were averaged and energy calibrated using ProXAS in house software and background corrected and normalised using the Athena program from the Demeter software suite. Fourier transformation of EXAFS data was performed using k^2 weightings in the range of 3-12 $Å^{-1}$.

Fourier Transformed Infrared spectroscopy (FT-IR) measurements were carried out using a Bruker INVENIO-R FT-IR Spectrometer equipped with a diamond ATR crystal. Ultraviolet-visible (UV-vis) measurements of the polymers were carried out in a dispersion of dichloromethane using a quartz cuvette in a Cary 60 UV-Vis spectrophotometer. Fluorescence quenching experiments as well as fluorescence spectra of the polymers were performed in an aqueous dispersion (1% v/v NMP) using a Tecan Infinite 200 PRO plate reader.

Author Contributions

M.A.R.-C. and B.M. conceived the project and wrote the manuscript, M.A.R.-C. performed the mechanistic studies, synthesis and characterisation of the polymers and their applications, M.A.R.-C. and G.T. carried out the application of the materials in heterogeneous catalysis, all authors contributed to the manuscript and the SI.

ACKNOWLEDGMENTS

The authors thank ETH and the European Research Council under the European Union's Horizon 2020 research and innovation program (Shuttle Cat, Project ID: 757608) for funding. This publication was created as part of NCCR Catalysis, a National Centre of Competence in Research funded by the Swiss National Science Foundation. M.A.R.-C. thanks Fundación Ramón Areces for a fellowship. G.T. thanks Studienstiftung des deutschen Volkes for a scholarship. ScopeM, SMOOC, Dr. René Verel and Prof. Copéret are acknowledged for providing access to electron microscopy, powder XRD, solid state NMR and physisorption instruments, respectively. We thank Dr. Olga Safonova (PSI) for her assistance in the XAS experiments. Ori Green, Marius Lutz and Michael Bogdos from Prof. Morandi's group are acknowledged for their help in XAS measurements. We acknowledge the Morandi group members for critical proofreading of this manuscript.

REFERENCES

1 Feng, X., Ding, X. & Jiang, D. Covalent organic frameworks. *Chem. Soc. Rev.* **41**, 6010-6022, doi:10.1039/c2cs35157a (2012).

2 Ding, S. Y. & Wang, W. Covalent organic frameworks (COFs): from design to applications. *Chem. Soc. Rev.* **42**, 548-568, doi:10.1039/c2cs35072f (2013).

3 Segura, J. L., Mancheno, M. J. & Zamora, F. Covalent organic frameworks based on Schiff-base chemistry: synthesis, properties and potential applications. *Chem. Soc. Rev.* **45**, 5635-5671, doi:10.1039/c5cs00878f (2016).

4 Zhu, L. & Zhang, Y. B. Crystallization of Covalent Organic Frameworks for Gas Storage Applications. *Molecules* **22**, doi:10.3390/molecules22071149 (2017).

5 Wang, J. & Zhuang, S. Covalent organic frameworks (COFs) for environmental applications. *Coord. Chem. Rev.* **400**, doi:10.1016/j.ccr.2019.213046 (2019).

6 Zhao, X. *et al.* Macro/Microporous Covalent Organic Frameworks for Efficient Electrocatalysis. *J. Am. Chem. Soc.* **141**, 6623-6630, doi:10.1021/jacs.9b01226 (2019).

7 Rodriguez-San-Miguel, D. & Zamora, F. Processing of covalent organic frameworks: an ingredient for a material to succeed. *Chem. Soc. Rev.* **48**, 4375-4386, doi:10.1039/c9cs00258h (2019).

8 Wang, Z., Zhang, S., Chen, Y., Zhang, Z. & Ma, S. Covalent organic frameworks for separation applications. *Chem. Soc. Rev.* **49**, 708-735, doi:10.1039/c9cs00827f (2020).

9 Geng, K. *et al.* Covalent Organic Frameworks: Design, Synthesis, and Functions. *Chem. Rev.* **120**, 8814-8933 doi:10.1021/acs.chemrev.9b00550 (2020).

10 Kaur, P., Hupp, J. T. & Nguyen, S. T. Porous Organic Polymers in Catalysis: Opportunities and Challenges. *ACS Catal.* **1**, 819-835, doi:10.1021/cs200131g (2011).

11 Byun, Y., Je, S. H., Talapaneni, S. N. & Coskun, A. Advances in Porous Organic Polymers for Efficient Water Capture. *Chem. Eur. J.* **25**, 10262-10283, doi:10.1002/chem.201900940 (2019).

12 Díaz, U. & Corma, A. Ordered covalent organic frameworks, COFs and PAFs. From preparation to application. *Coord. Chem. Rev.* **311**, 85-124, doi:10.1016/j.ccr.2015.12.010 (2016).

13 Lee, J. M. & Cooper, A. I. Advances in Conjugated Microporous Polymers. *Chem. Rev.* **120**, 2171-2214, doi:10.1021/acs.chemrev.9b00399 (2020).

14 Wang, W. & Schlüter, A. D. Synthetic 2D Polymers: A Critical Perspective and a Look into the Future. *Macromol. Rapid Commun.* **40**, 1800719, doi:10.1002/marc.201800719 (2019).

15 Jin, Y., Wang, Q., Taynton, P. & Zhang, W. Dynamic covalent chemistry approaches toward macrocycles, molecular cages, and polymers. *Acc. Chem. Res.* **47**, 1575-1586, doi:10.1021/ar500037v (2014).

16 Zhu, J.-B., Watson, E. M., Tang, J. & Chen, E. Y.-X. A synthetic polymer system with repeatable chemical recyclability. *Science* **360**, 398-403, doi:10.1126/science.aar5498 (2018).

17 Rahate, A. S., Nemade, K. R. & Waghuley, S. A. Polyphenylene sulfide (PPS): state of the art and applications. *Rev. Chem. Eng.* **29**, doi:10.1515/revce-2012-0021 (2013).

18 Zuo, P., Tcharkhtchi, A., Shirinbayan, M., Fitoussi, J. & Bakir, F. Overall Investigation of Poly (Phenylene Sulfide) from Synthesis and Process to Applications—A Review. *Macromol. Mater. Eng.* **304**, 1800686, doi:10.1002/mame.201800686 (2019).

19 Horiuchi, S. *et al.* Well-Controlled Synthesis of Poly (phenylene sulfide) (PPS) Starting from Cyclic Oligomers. *Macromol. Symp.* **349**, 9-20, doi:10.1002/masy.201300221 (2015).

20 Van Bierbeek, A. & Gingras, M. Polysulfurated branched molecules containing functionalized m-phenylene sulfides. *Tetrahedron Lett.* **39**, 6283-6286, doi:https://doi.org/10.1016/S0040-4039(98)01327-6 (1998).

21 Cao, Y. *et al.* Porous Organic Polymers Containing a Sulfur Skeleton for Visible Light Degradation of Organic Dyes. *Chem.: Asian J.* **14**, 2883-2888, doi:10.1002/asia.201900477 (2019).

22 Ong, W. J. & Swager, T. M. Dynamic self-correcting nucleophilic aromatic substitution. *Nat. Chem.* **10**, 1023-1030, doi:10.1038/s41557-018-0122-8 (2018).

23 Lian, Z., Bhawal, B. N., Yu, P. & Morandi, B. Palladium-catalyzed carbon-sulfur or carbon-phosphorus bond metathesis by reversible arylation. *Science* **356**, 1059-1063, doi:10.1126/science.aam9041 (2017).

24 Delcaillau, T., Bismuto, A., Lian, Z. & Morandi, B. Nickel-Catalyzed Inter- and Intramolecular Aryl Thioether Metathesis by Reversible Arylation. *Angew. Chem. Int. Ed.* **59**, 2110-2114, doi:10.1002/anie.201910436 (2020).

25 Chen, Y., Abdellatif, M. M. & Nomura, K. Olefin metathesis polymerization: Some recent developments in the precise polymerizations for synthesis of advanced materials (by ROMP, ADMET). *Tetrahedron* **74**, 619-643, doi:https://doi.org/10.1016/j.tet.2017.12.041 (2018).

26 Sutthasupa, S., Shiotsuki, M. & Sanda, F. Recent advances in ring-opening metathesis polymerization, and application to synthesis of functional materials. *Polym. J.* **42**, 905-915, doi:10.1038/pj.2010.94 (2010).

27 Matsumoto, M. *et al.* Rapid, Low Temperature Formation of Imine-Linked Covalent Organic Frameworks Catalyzed by Metal Triflates. *J. Am. Chem. Soc.* **139**, 4999-5002, doi:10.1021/jacs.7b01240 (2017).

28 Zhu, Y., Yang, H., Jin, Y. & Zhang, W. Porous Poly(aryleneethynylene) Networks through Alkyne Metathesis. *Chem. Mater.* **25**, 3718-3723, doi:10.1021/cm402090k (2013).

29 Yang, H. *et al.* Aromatic-rich hydrocarbon porous networks through alkyne metathesis. *Mater. Chem. Front.* **1**, 1369-1372, doi:10.1039/c6qm00359a (2017).

30 Feriante, C. H. *et al.* Rapid Synthesis of High Surface Area Imine-Linked 2D Covalent Organic Frameworks by Avoiding Pore Collapse During Isolation. *Adv. Mater.* **32**, e1905776, doi:10.1002/adma.201905776 (2020).

31 Smith, B. J. *et al.* Colloidal Covalent Organic Frameworks. *ACS Cent. Sci.* **3**, 58-65, doi:10.1021/acscentsci.6b00331 (2017).

32 Beck, H. N. Process for forming articles comprising poly (phenylene sulfide)(PPS). US5043112 (1991).

33 Flahive, E. *et al.* A High-Throughput Methodology for Screening Solution-Based Chelating Agents for Efficient Palladium Removal. *QSAR Comb. Sci.* **26**, 679-685, doi:10.1002/qsar.200610124 (2007).

34 Bismuto, A., Delcaillau, T., Müller, P. & Morandi, B. Nickel-Catalyzed Amination of Aryl Thioethers: A Combined Synthetic and Mechanistic Study. *ACS Catal.* **10**, 4630-4639, doi:10.1021/acscatal.0c00393 (2020).

35 Guan, X. *et al.* Chemically stable polyarylether-based covalent organic frameworks. *Nat. Chem.* **11**, 587-594, doi:10.1038/s41557-019-0238-5 (2019).

36 Ravindra, K., Bencs, L. & Van Grieken, R. Platinum group elements in the environment and their health risk. *Sci. Total Environ.* **318**, 1-43, doi:https://doi.org/10.1016/S0048-9697(03)00372-3 (2004).

37 Li, H., Fan, J. & Peng, X. Colourimetric and fluorescent probes for the optical detection of palladium ions. *Chem. Soc. Rev.* **42**, 7943-7962, doi:10.1039/C3CS60123D (2013).

38 Wang, M., Yuan, Y., Wang, H. & Qin, Z. A fluorescent and colorimetric probe containing oxime-ether for Pd^{2+} in pure water and living cells. *Analyst* **141**, 832-835, doi:10.1039/C5AN02225H (2016).

39 Duan, L., Xu, Y. & Qian, X. Highly sensitive and selective Pd^{2+} sensor of naphthalimide derivative based on complexation with alkynes and thio-heterocycle. *Chem. Commun.*, 6339-6341, doi:10.1039/B815298E (2008).

40 Yang, P., Shu, Y., Zhuang, Q., Li, Y. & Gu, J. A robust MOF-based trap with high-density active alkyl thiol for the super-efficient capture of mercury. *Chem. Commun.* **55**, 12972-12975, doi:10.1039/c9cc06255f (2019).

41 Huang, N., Zhai, L., Xu, H. & Jiang, D. Stable Covalent Organic Frameworks for Exceptional Mercury Removal from Aqueous Solutions. *J. Am. Chem. Soc.* **139**, 2428-2434, doi:10.1021/jacs.6b12328 (2017).

42 Hong, Y. *et al.* Precious metal recovery from electronic waste by a porous porphyrin polymer. *Proc. Natl. Acad. Sci. U.S.A.* **117**, 16174-16180, doi:10.1073/pnas.2000606117 (2020).

43 La, D. D., Bhosale, S. V., Jones, L. A. & Bhosale, S. V. Tetraphenylethylene-Based AIE-Active Probes for Sensing Applications. *ACS Appl. Mater. Interfaces* **10**, 12189-12216, doi:10.1021/acsami.7b12320 (2018).

44 Kowser, Z., Rayhan, U., Akther, T., Redshaw, C. & Yamato, T. A brief review on novel pyrene based fluorometric and colorimetric chemosensors for the detection of Cu2+. *Mater. Chem. Front.* **5**, 2173-2200, doi:10.1039/D0QM01008A (2021).

45 Bowron, D. T., Beret, E. C., Martin-Zamora, E., Soper, A. K. & Sánchez Marcos, E. Axial Structure of the Pd(II) Aqua Ion in Solution. *J. Am. Chem. Soc.* **134**, 962-967, doi:10.1021/ja206422w (2012).

46 Liu, B. *et al.* Synthesis and characterization of a fluorescent polymer containing 2,6-bis(2-thienyl)pyridine moieties as a highly efficient sensor for Pd^{2+} detection. *Chem. Commun.* **47**, 1731-1733, doi:10.1039/C0CC03819A (2011).

47 Helal, A., Nguyen, H. L., Al-Ahmed, A., Cordova, K. E. & Yamani, Z. H. An Ultrasensitive and Selective Metal–Organic Framework Chemosensor for Palladium Detection in Water. *Inorg. Chem.* **58**, 1738-1741, doi:10.1021/acs.inorgchem.8b02871 (2019).

48 Cai, S. *et al.* A highly sensitive and selective turn-on fluorescent chemosensor for palladium based on a phosphine–rhodamine conjugate. *Chem. Commun.* **49**, 822-824, doi:10.1039/C2CC37746B (2013).

49 Vile, G. *et al.* A stable single-site palladium catalyst for hydrogenations. *Angew. Chem. Int. Ed.* **54**, 11265-11269, doi:10.1002/anie.201505073 (2015).

50 Chen, Z. *et al.* A heterogeneous single-atom palladium catalyst surpassing homogeneous systems for Suzuki coupling. *Nat. Nanotechnol.* **13**, 702-707, doi:10.1038/s41565-018-0167-2 (2018).

51 Lee, S. *et al.* Dynamic metal-polymer interaction for the design of chemoselective and long-lived hydrogenation catalysts. *Sci. Adv.* **6**, eabb7369, doi:10.1126/sciadv.abb7369 (2020).

52 Albani, D. *et al.* Selective ensembles in supported palladium sulfide nanoparticles for alkyne semi-hydrogenation. *Nat. Commun.* **9**, 2634, doi:10.1038/s41467-018-05052-4 (2018).

53 Huang, X. *et al.* Toward Understanding of the Support Effect on Pd1 Single-Atom-Catalyzed Hydrogenation Reactions. *J. Phys. Chem. C* **123**, 7922-7930, doi:10.1021/acs.jpcc.8b07181 (2019).

54 Coates, G. W. & Getzler, Y. D. Y. L. Chemical recycling to monomer for an ideal, circular polymer economy. *Nat. Rev. Mater.* **5**, 501-516, doi:10.1038/s41578-020-0190-4 (2020).

55 Gross, D. E., Discekici, E. & Moore, J. S. Macrocyclic depolymerization of arylene-ethynylene copolymers: a dynamic combinatorial method. *Chem. Commun.* **48**, 4426-4428, doi:10.1039/c2cc30701d (2012).

56 Chavez, A. D. *et al.* Equilibration of Imine-Linked Polymers to Hexagonal Macrocycles Driven by Self-Assembly. *Chemistry* **24**, 3989-3993, doi:10.1002/chem.201800459 (2018).